A Study of the Reactive Intermediate IF and I Atoms with Photoelectron Spectroscopy

Fabrizio Innocenti,[†] Marie Eypper,[†] Sonya Beccaceci,[†] Alan Morris,[†] Stefano Stranges,[‡] John B. West,[§] George C. King,*[,||] and John M. Dyke*[,†]

Department of Chemistry, University of Southampton, Highfield, Southampton SO17 1BJ, U.K., Department of Chemistry and INSTM Unit, "La Sapienza", University of Rome, Italy, ISNM-CNR sez. Roma La Sapienza and Laboratorio TASC-INFM-CNR, Trieste, Italy, STFC Daresbury Laboratory, Daresbury, Warrington WA4 4AD, U.K., and Department of Physics, Manchester University, Manchester M13 9PL, U.K.

Received: April 11, 2008

Angle-resolved photoelectron (PE) spectra were recorded for IF and I. These were prepared as primary and secondary products of the $F + CH_2I_2$ reaction. PE spectra were recorded with different IF-to-I ratios to evaluate the relative intensities of IF and I photoelectron bands where their bands were overlapped. Improved values were obtained for the vertical and adiabatic ionization energies of the $IF^+(X^2\Pi_{3/2}) \leftarrow IF(X^1\Sigma^+)$ and $IF^+(^2\Pi_{1/2}) \leftarrow IF(X^1\Sigma^+)$ ionizations and for the spectroscopic constants ω_e and $\omega_e x_e$ for the two IF ionic states $X^2\Pi_{3/2}$ and $^2\Pi_{1/2}$. Equilibrium bond lengths r_e of these IF ionic states were derived from the experimental relative intensities of the vibrational components and calculated Franck−Condon factors. Threshold photoelectron (TPE) spectra were also recorded under the same reaction conditions. On comparing the TPE and PE spectra, the contributions from atomic iodine were much more intense in the TPE spectra. No difference was seen between the vibrational envelopes of the two observed IF bands, and no extra structure was seen associated with the TPE bands of IF as has been observed in TPE spectra of other diatomic halogens. The extra features that were observed in the TPE spectra can be assigned to contributions from autoionization of known I Rydberg states.

Introduction

This article reports a study of I and IF by photoelectron spectroscopy (PES) and threshold photoelectron spectroscopy (TPES). Iodine is a reactive open-shell atom, and investigating its photoionization behavior and measurement of its partial photoionization cross sections should provide valuable information that will allow comparison between theory and experiment, and hence enable testing of the theoretical methods used. Also, a study of IF with these methods will allow its valence ionization energies and low-lying ionic state spectroscopic constants to be established. IF is a short-lived molecule in the gas phase that typically has a lifetime of several milliseconds in a low pressure flowing gas system. It has been shown to be a promising candidate for a visible chemical laser via energy transfer to its vibrationally excited ground state, $IF(X^1\Sigma^+)$, from $O_2(a^1\Delta_g)$ to produce $IF(B^3\Pi)$.[1–3]

Although an initial investigation of IF with PES has been made,[4] the higher resolution threshold photoelectron spectrum has not yet been obtained. PES and TPES are complementary methods of studying the electronic structure and spectroscopy of molecular ions. The PE and TPE spectra of the stable halogens and interhalogens F_2, Cl_2, Br_2, ICl, and IBr have been recorded previously.[5–8] In these cases, the TPE spectra are notable in that extra vibrational structure is observed in the Franck−Condon gaps between the PE bands. Also, in the TPE spectra the resolution is higher than that in PES. In TPES, the resolution is limited by the resolution of the scanned photon source (typically 1−3 meV for a synchrotron source) combined with the low energy (threshold) electrons selected (typically below 3 meV), whereas in UV PES the resolution (typically 25 meV) is governed by the geometrical characteristics of the energy analyzer used. In the initial study of IF by PES,[4] IF was produced from the rapid gas-phase reaction $F + ICl \rightarrow IF + Cl$. However, because of the minor reaction channel $F + ICl \rightarrow FCl + I$, I atoms were also observed in the spectra and some of the I atom features overlapped with some of the vibrational components in the first two IF PE bands. For these overlapped bands, the relative contributions of I and IF were not established.

The main objective of this work therefore was to determine these contributions. In this way, reliable vibrational envelopes of the PE bands of IF and the relative intensities of I atom bands will be obtained. The $F + CH_2I_2$ reaction was studied at different reactant times to obtain PE spectra with different partial pressures of I and IF in the photoionization region. These spectra were then used to obtain "pure" PE spectra of both I and IF. Once the PE spectra had been obtained, TPE spectra were then recorded.

Experimental Section

The experiments reported here were undertaken on the Circularly Polarized Beamline (4.2R, Polar) at the Elettra synchrotron radiation source using a photoelectron spectrometer that was specifically designed to study reactive intermediates.[9–11] PE spectra were recorded as described in the earlier work,[12] and the same procedures were used to normalize the spectra for photon flux and the transmission function of the spectrometer. Most spectra were recorded at the angle of 54° 44′ with respect to the direction of polarization of the photon beam. At this angle, the measured PE intensity is proportional to the photoionization cross section and is independent of the angular

* Authors to whom correspondence should be addressed.
[†] University of Southampton.
[‡] University of Rome and ISNM-CNR sez. Roma La Sapienza and Laboratorio TASC-INFM-CNR.
[§] STFC Daresbury Laboratory.
[||] Manchester University.

10.1021/jp803141c CCC: $40.75
Published on Web 07/10/2008

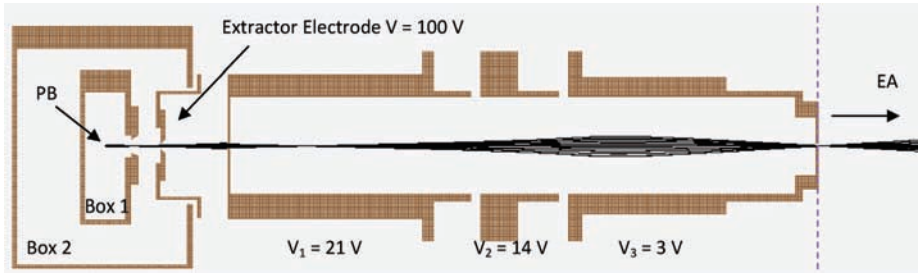

Figure 1. Simulations of trajectories of 1 meV photoelectrons. PB denotes the photon beam, which is at right angles to the plane shown. EA shows electrons entering the 180° hemispherical analyzer.

distribution parameter β. The resolution of the PE spectra is ~35 meV. This is determined mainly by the slit widths and the mean radius of the hemispherical analyzer used. Because of the DAC card used to supply the voltages to the lenses of the spectrometer, excellent linearity and reproducibility of the ionization energy scale was obtained in PE spectra. This allowed band maxima to be measured to within 1 meV (see later).

The spectrometer was modified so that TPE spectra could also be recorded. This was achieved by adding an extra electrode between the ionization region and the lens system of the photoelectron spectrometer. A potential applied to this electrode generates a penetrating field[13] in the interaction region that selectively extracts low-energy (threshold) electrons. The technique results in a very large solid angle of collection (~4π sr) for low-energy electrons, ≤10 meV, while more energetic electrons are discriminated against. It also produces a crossover point or focus of electron trajectories that acts as input to the following lens system. The geometry was optimized by simulating computed electron trajectories for threshold electrons from the photoionization region through the three element lens to the entrance of the 180° hemispherical electron energy analyzer. Figure 1 shows a simulation of trajectories of 1 meV photoelectrons with an extractor potential of 100 V and electrostatic lens potentials of $V_1 = 21$ V, $V_2 = 14$ V, and $V_3 = 3$ V. The last lens voltage, V_3, is set equal to the pass energy of the hemispherical analyzer. These simulations also show that the entrance slit of 1 mm in the first lens further discriminates against more energetic electrons (≥2 meV). Some energetic electrons with initial trajectories along the axis of the lens system may pass through the extractor and the lens system. These are discriminated against by the hemispherical electron energy analyzer (not shown in Figure 1) and are not detected. The combination of the field penetration stage and the hemispherical analyzer gives an overall transmission function that is sharply peaked for threshold electrons and falls off rapidly with electron kinetic energy.

TPES differs from PES in that the energy of the detected electrons is kept low (typically <2 meV) while the photon energy is scanned. A threshold photoelectron signal will be obtained each time the photon energy is equal to the ionization energy to an ionic state. While the observed intensities of vibrational components in a conventional PE spectrum are almost always governed by Franck−Condon factors (FCFs) between the initial neutral and final ionic state, those observed by TPES are often dominated by autoionization.[14,15] This is primarily due to the high density of Rydberg states which are parts of series that converge on higher rovibronic ionic levels, some of which can lie just above a selected ionization threshold. These can autoionize and produce electrons of low kinetic energy that are detected in TPES. In many cases, the autoionization process can enable the observation of ionic states that cannot be observed by direct ionization from the ground state in conventional PES or can allow extra vibrational components of an ionic state, seen in PES, to be observed in TPES.

In this work, I atoms and IF were produced by the rapid reaction of F atoms with CH_2I_2:[16]

$$\text{Primary reaction: } F + CH_2I_2 \rightarrow CH_2I + IF$$

$$\text{Subsequent reactions: } F + CH_2I \rightarrow [CH_2IF]^{\dagger} \rightarrow CH_2F + I$$

$$\rightarrow CHF + HI$$

$$CH_2I + CH_2I \rightarrow [CH_2ICH_2I]^{\dagger} \rightarrow HI + CH_2CHI$$

In an earlier PES study of the F + CH_2I_2 reaction by the Southampton group,[17] CH_2I was observed at low mixing distances (~0.3 cm) (at 8.52 eV vertical ionization energy (VIE)), whereas only bands from I, IF, HI, HF, and CH_2CHI (vinyl iodide), and CF (weakly) were observed at longer mixing distances (~3−4 cm), corresponding to the conditions used in the present work. It is clear that the reactive intermediates CH_2F and CHF in the above reaction sequence are converted to CF + HF at the relatively long reaction times used in this work.

A high yield of fluorine atoms was produced by flowing 5% F_2 in helium through a microwave discharge at 2.45 GHz in the side arm of a glass inlet system, as described previously.[9−11] This system also has an inner inlet system that is used to transport the target reaction molecule (in this case CH_2I_2) to the reaction region. To minimize attack of the glass system by the fluorine atoms, the inner surfaces of both the tubes were coated with a thin layer of Teflon. In addition, the discharge cavity was positioned on an alumina section of the inlet system to prevent melting of the Teflon because of heating from the discharge.[9−11]

Preliminary experiments were carried out in Southampton to determine the optimum pressures and reactant mixing distances above the photon beam that maximize the intensities of the I and IF features in the PE spectra. The optimum partial pressures were: $\Delta p(CH_2I_2) = 1 \times 10^{-6}$, $\Delta p(F_2/He) = 5 \times 10^{-6}$, and $\Delta p(Ar) = 3 \times 10^{-7}$ mbar. These partial pressures were determined using an ionization gauge connected to the main vacuum chamber and were measured with respect to the background pressure in the vacuum chamber (1×10^{-7} mbar). The argon gas was introduced to allow optimization of the electrode voltages when TPE spectra were recorded, as described below. The most intense spectra of the I bands were obtained at a mixing distance of about 4 cm from the photon beam, while the IF bands were optimized at a shorter mixing distance of about 3 cm.

Results and Discussion

The interhalogen IF has the electronic configuration $-12\sigma^2 6\pi^4 13\sigma^2 7\pi^4$. In the initial study of this reactive intermediate with PES using He Iα radiation,[4] where IF was prepared using

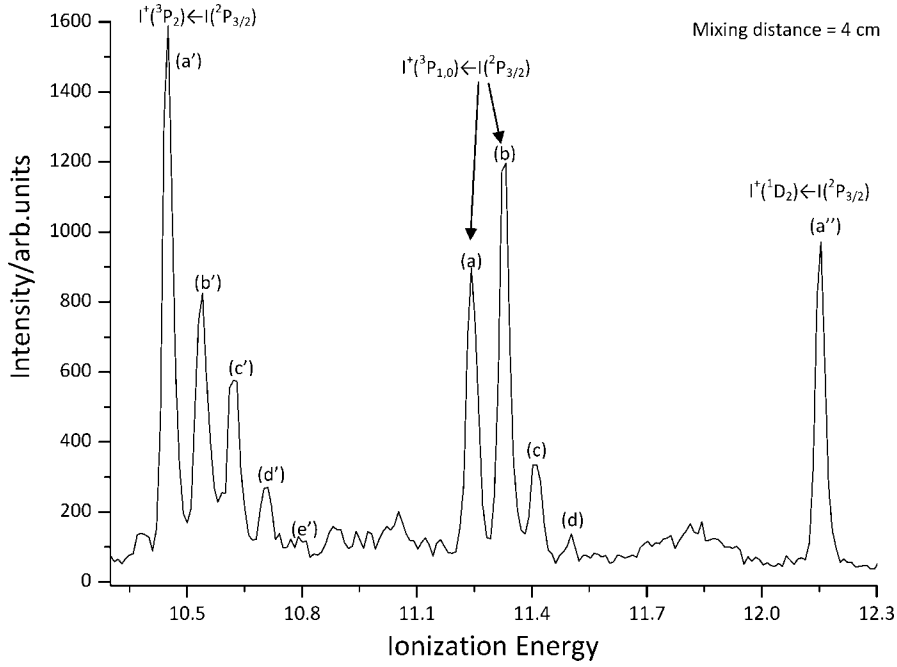

Figure 2. PE spectrum recorded at hν = 21.22 eV at 54°44′ and 4 cm mixing distance from the photon beam showing a "high" I-to-IF ratio.

the F + ICl reaction, the first two bands were vibrationally resolved. They correspond to ionization to the $^2\Pi_{3/2}$ and $^2\Pi_{1/2}$ ionic states at VIEs of 10.62 and 11.32 eV, respectively, arising from the $(7\pi)^{-1}$ ionization. The $(13\sigma)^{-1}$ and $(6\pi)^{-1}$ ionizations gave rise to broad bands at VIEs of 15.22 and 15.94 eV, respectively, which showed no vibrational structure.[4]

The ground-state electronic configuration of atomic iodine is ---$5s^25p^5$. This gives rise to two states, $^2P_{3/2}$ and $^2P_{1/2}$, separated by 0.94 eV with the $^2P_{3/2}$ state lower.[18] The $^2P_{1/2}$ state is effectively not populated under equilibrium conditions at room temperature. I atoms were first observed by PES by de Leeuw and co-workers,[18] where a partial photoelectron spectrum was obtained. The $(5p)^{-1}$ ionization from the $^2P_{3/2}$ ground state is expected to give $^3P_2$, $^3P_1$, $^3P_0$, $^1D_2$, and $^1S_0$ ionic states with the following ionization energies determined from photoabsorption measurements:[19,20]

$$I^+(^3P_2) \leftarrow I(^2P_{3/2}) \quad 10.451 \text{ eV}$$
$$I^+(^3P_0) \leftarrow I(^2P_{3/2}) \quad 11.251 \text{ eV}$$
$$I^+(^3P_1) \leftarrow I(^2P_{3/2}) \quad 11.330 \text{ eV}$$
$$I^+(^3D_2) \leftarrow I(^2P_{3/2}) \quad 12.153 \text{ eV}$$
$$I^+(^1S_0) \leftarrow I(^2P_{3/2}) \quad 14.109 \text{ eV}$$

The $(5s)^{-1}$ ionization, which was not studied in this work, gives $^3P_{2,1,0}$ and $^1P_1$ ionic states, respectively, with ionization energies 20.61, 20.89, 21.66, and 23.35 eV, respectively.[19]

a. Photoelectron Spectra. Figures 2 and 3 show PE spectra recorded for the F + CH_2I_2 reaction, in the region from 10.3 to 12.3 eV with mixing distances of 4 and 3 cm, respectively. The selected photon energy using the synchrotron source was 21.22 eV, and the spectra were recorded at the angle of θ = 54° 44′. In the spectrum recorded at 4-cm mixing distance (Figure 2), the intensities of the atomic I spectral features compared to those of the IF features are higher than in the spectrum recorded at 3-cm mixing distance (Figure 3).

As shown in these spectra, two groups of bands were observed in the regions 10.35−10.80 and 11.25−11.55 eV with a single band at 12.15 eV. To assist the analysis and discussion, these were labeled (a′−e′), (a−d), and a″ as shown.

The assignment of the bands shown in Figures 2 and 3 is as reported in the initial study of IF using He I photoelectron spectroscopy,[7] where the IF was produced from the reaction F + ICl. In brief, bands (b′) to (e′) are vibrational components of the first IF band, bands (a) to (d) are vibrational components of the second IF band, and I atom ionizations are as labeled in Figure 2. However, for some of the observed features, such as features (a) and (b), the relative contribution from I and IF is not known. It is also not known whether IF contributes to band (a′).

The spectra shown in Figures 2 and 3 were normalized in intensity to the pure IF vibrational feature (c′). Gaussian fitting was used to obtain the relative areas of all the bands. This approach was also used to analyze the many PE spectra recorded (∼20) with different I-to-IF ratios. Spectra with different I/IF ratios were obtained by recording PE spectra at different mixing distances and at selected atomic iodine resonance photon energies. The resonance positions to excited atomic Rydberg states were obtained by recording constant ionic state (CIS) spectra on the first and fourth PE bands of I atoms. It was also possible to obtain different I/IF ratios at the same mixing distance by recording PE spectra at different times (e.g., when the reaction had just been started and after the reaction had been running for some time). This was possible since the I atom intensity decreased with respect to IF over the time scale of several hours, probably because of the change in efficiency in wall recombination of I atoms with time. Many spectra with different I-to-IF ratios were recorded during the several days that the reaction was running.

Once each PE spectrum had been normalized in intensity to band (c′), an IF vibrational component, spectra were selected in pairs for analysis: one spectrum with "high" I atom intensity and another spectrum with "low" I atom intensity. The procedure used can be illustrated by considering Figures 2 and 3. The band intensity ratio was calculated for each band by dividing the area of each band in Figure 2 by the area of the corresponding band in Figure 3. This is expected to be equal to 1.0 for a pure IF

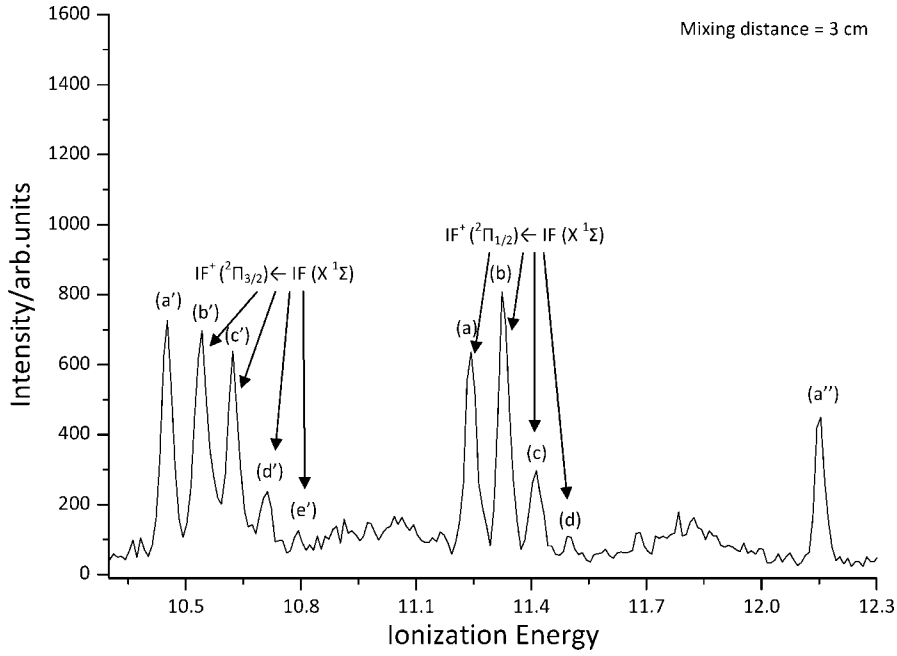

Figure 3. PE spectrum recorded at hν = 21.22 eV at 54°44′ and 3 cm mixing distance above the photon beam showing a "low" I-to-IF ratio.

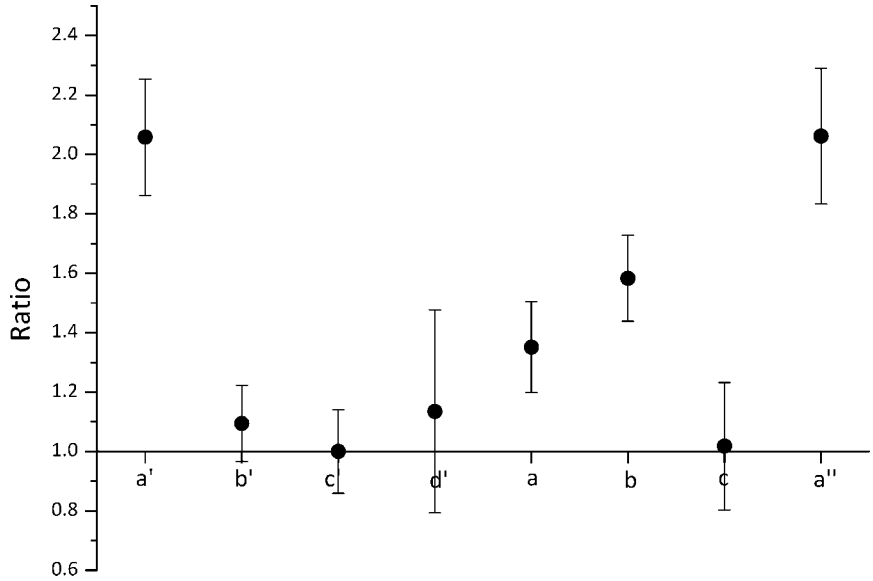

Figure 4. Band intensity ratio calculated by dividing the area of the more intense ionic bands in Figure 2 by the area of the same bands in Figure 3 after the intensity of band (c′) was made the same in both spectra (see text).

band. Since band (a″) corresponds to the pure $I^+(^1D_2) \leftarrow I(^2P_{3/2})$ ionization, the ratio calculated for this band gives the increase (or decrease) of the I atoms between the two spectra. Figure 4 shows the ratio for the observed bands calculated by dividing the areas obtained in the spectrum in Figure 2 with respect to the areas obtained in the spectrum in Figure 3 after the intensity of band (c′) was made the same in both spectra. The error associated with each ratio is also reported. All the ratios obtained from analysis of all the PE spectra recorded give a pattern similar to that shown in Figure 4. First, it can be seen that, as expected, bands (b′), (c′), (d′), and (c) are pure IF bands since their ratio is equal to 1.0 within the error associated with the measurement. Band (a′) has the same ratio as the $I^+(^1D_2) \leftarrow I(^2P_{3/2})$ band, band (a″), indicating that (a′) is a pure I band or that the contribution of IF to band (a′) is so small that it cannot be determined with this procedure. The ratios for bands (a) and (b) are bigger than 1.0 (when the experimental errors for the ratios of bands (a) and (b) are considered) but smaller than that obtained for a pure I band, band (a″). Therefore, bands (a) and (b) have contributions from both I and IF, as expected because of known I atom ionizations in these positions. It can be seen that band (b) has a bigger contribution of I with respect to band (a).

Taking band (a) as an example, which contains contributions from I and IF, and assuming the I atom ratio in Figure 4 for band (a) is the same as that of the pure I atom band (a″) (or band (a′)), it is possible to separate the contribution of I and IF in band (a). The same procedure can be used for band (b). It is assumed that $Area_1$ and $Area_2$ are the areas of band (a) in Figures 2 and 3 (after normalizing the two spectra to ensure areas of band (c) are the same), $Area_{IF}$ is the area of the IF contribution, and I_1 and I_2 are the I contributions to band (a) in the two

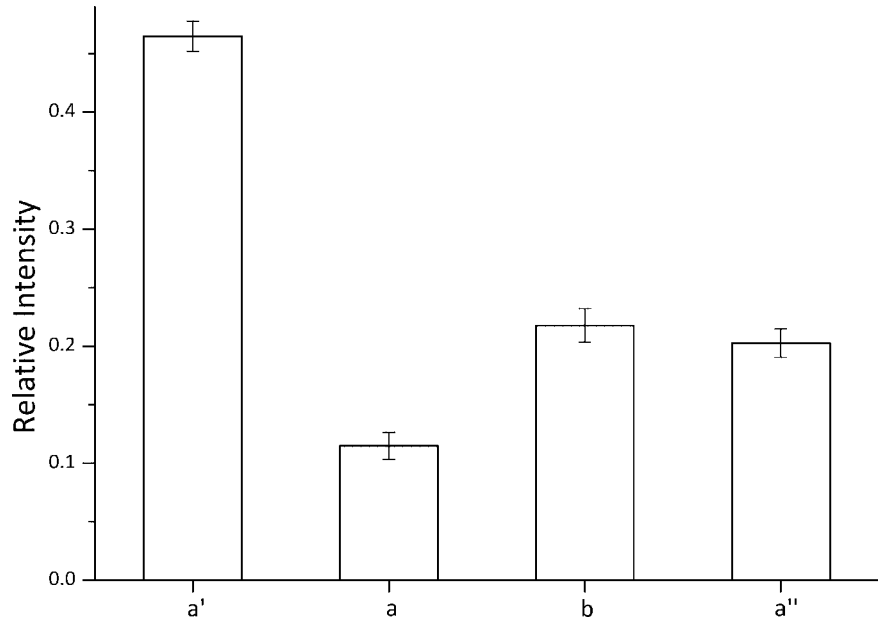

Figure 5. Relative intensities of the four iodine atom components, derived using the procedure described in the text.

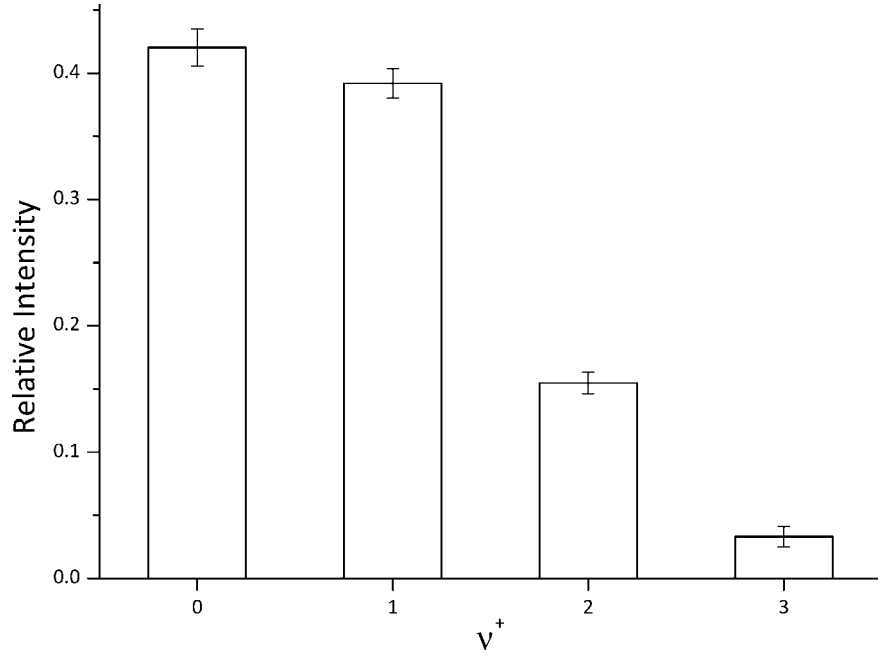

Figure 6. Relative intensities obtained for the IF components in the $IF^+(X^2\Pi_{3/2}) \leftarrow IF(X^1\Sigma)$ band.

spectra. The ratio I_1/I_2 is then set equal to the ratio of band (a″) or alternatively of band (a′) as both are pure I atom bands. Then, using

$$\text{Area}_1 = I_1 + \text{Area}_{IF}$$
$$\text{Area}_2 = I_2 + \text{Area}_{IF}$$
$$\text{Ratio} = I_1/I_2 = \text{Ratio}(\alpha')$$
$$I_2 = \frac{\text{Area}_1 - \text{Area}_2}{(\text{Ratio} - 1)}$$
$$I_1 = I_2 \times \text{Ratio}$$

knowing Ratio, Area_1 and Area_2, I_1 and I_2 can be calculated, and hence Area_{IF} can be calculated. The same calculation can be applied to band (b) allowing the determination in each spectrum of the relative intensities of the four I atom bands (at positions of bands a′, a, b, and a″) as well as the relative intensities of the IF vibrational bands. The same procedure was used for any two PE spectra with different I-to-IF ratios from all the PE spectra recorded. All the relative intensities so obtained were averaged, and the results are shown in Figures 5, 6, and 7.

The relative intensities of iodine atom bands obtained in this work, including that measured for the $I^+(^1S_0) \leftarrow I(^2P_{3/2})\ (5p)^{-1}$ ionization at 14.109 eV not shown in Figures 2 and 3, can be compared with those obtained in refs[21] and[22] by PES with a He Iα (21.217 eV) photon source, as reported in Table 1. The results are quite similar within experimental error to the results obtained in refs[21] and[22] with the exception of the $I^+(^1D_2) \leftarrow I(^2P_{3/2})$ ionization. This has a much lower relative intensity in this work (0.58 ± 0.03 compared to the He Iα value in ref[21] of 0.80 ± 0.04) but is closer to the calculated value of refs[21] and[22] (0.57)

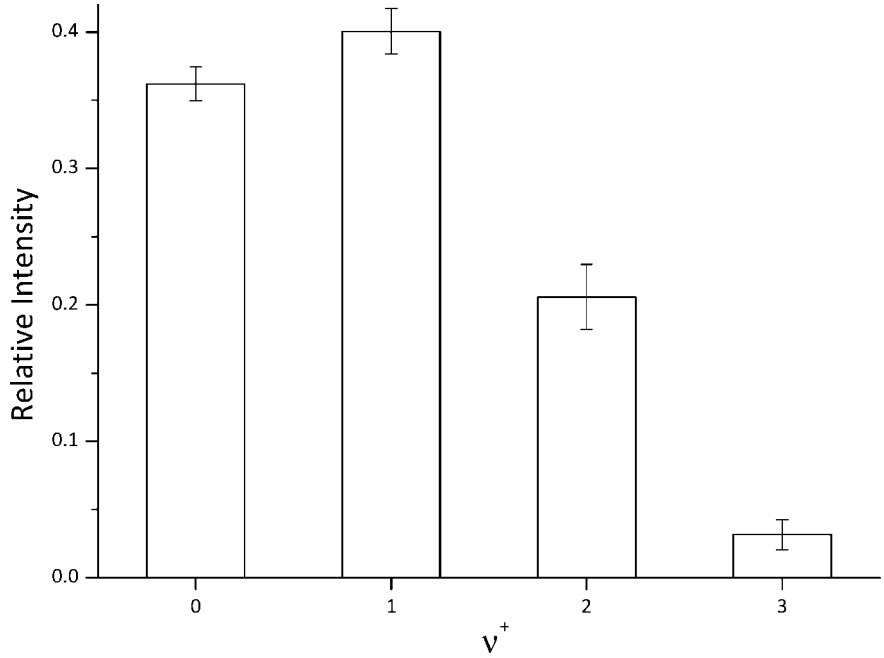

Figure 7. Relative intensities obtained for the IF components in the $IF^+(^2\Pi_{1/2}) \leftarrow IF(X^1\Sigma)$ band.

TABLE 1: Relative Intensities of Iodine Atoms Obtained in This Work Compared with Those in Refs 21 and 22

$I^+ \leftarrow I(^2P_{3/2})$ bands ionic state	ref 22[a]	ref 21[b]	this work, at $h\nu = 21.22$ eV
$^3P_2$	1.00 (1.00)	1.00 (1.00)	1.00 ± 0.03
$^3P_1$	0.34 (0.31)	0.39 ± 0.05 (0.31)	0.47 ± 0.03
$^3P_0$	0.17 (0.15)	0.18 ± 0.03 (0.15)	0.25 ± 0.02
$^1D_2$	0.79 (0.57)	0.80 ± 0.04 (0.57)	0.58 ± 0.03
$^1S_0$	0.06 (0.058)	0.04 ± 0.01 (0.05)	0.047 ± 0.005

[a] In ref,[22] I atoms were generated by heating solid silver iodide and relative intensities were obtained from a He Iα PE spectrum. The values in parentheses are relative intensities computed with an intermediate coupling model. [b] In ref,[21] I atoms were generated from the F + HI reaction and relative intensities were obtained from a He Iα PE spectrum. The values in parentheses are relative intensities computed with an intermediate coupling model.

using an intermediate coupling model. This difference can only be partly explained by considering the asymmetry parameter β for each ionization. The experimental work in refs[21] and[22] was carried out with unpolarized He Iα radiation, while the present results were obtained with linearly polarized radiation ($P > 0.99$), at the detection angle (54° 44′′) where the measured intensity is proportional to the total photoionization cross section and independent by β. Figure 8 shows the asymmetry parameter for the bands measured in the present work, and it can be clearly seen that the value of β is higher for the $I^+(^1D_2) \leftarrow I(^2P_{3/2})$ band (a′′) than for the $I^+(^3P_2) \leftarrow I(^2P_{3/2})$ band (a′). Relative cross section measurements depending on β would therefore give a higher relative intensity for $I^+(^1D_2) \leftarrow I(^2P_{3/2})$ ionization with respect to the present work. Indeed, the intensity of a band in a spectrum recorded with an unpolarized photon source and at an angle between the direction of the photoelectrons and the unpolarized radiation of 90°, as used in refs[21] and,[22] is proportional to the total photoionization cross section multiplied by a factor equal to $(1 + \beta/4)$.[23] Assuming $\beta = 1.01$ for band (a′) (the $I^+(^3P_2) \leftarrow I(^2P_{3/2})$ ionization) and 1.63 for band (a′′) (the $I^+(^1D_2) \leftarrow I(^2P_{3/2})$ ionization), then correcting for angular distribution, the relative intensity of bands (a′) to (a′′) changes from 0.80 (value from ref [21]) to 0.71. This value compares with 0.58 ± 0.03 derived in this work and 0.57 obtained using an intermediate coupling model.

PE spectral envelopes obtained at 21.22 eV for the two IF bands (Figures 6 and 7) were simulated by computing the FCFs between the ground state and the ionic state vibrational wave functions. To do this, the spectroscopic constants ω_e, $\omega_e x_e$, and r_e for each electronic state were used to generate a Morse potential for the IF and IF^+ states. Then the vibrational wave functions for each electronic state were obtained from numerical solutions of the vibrational Schrödinger equation with the appropriate potential. The vibrational constants used for the $IF(X^1\Sigma^+)$ state for the simulations were taken from a rotational and vibrational analysis of an electronic emission spectrum and from a microwave spectroscopic study.[24–26] The values used were: $\omega_e = 610.24\ cm^{-1}$, $\omega_e x_e = 3.123\ cm^{-1}$, and $r_e = 1.90975$ Å. The vibrational constants ω_e and $\omega_e x_e$ used for the ionic states were obtained by measuring the spacing (ΔE) between the IF vibrational components of each IF band. Since the equilibrium bond length of each ionic state is not known, a trial value must be used in the calculation of the FCFs. This trial value is chosen to be close to, although shorter than, the value of the neutral state. This is because in both IF bands, an electron has been removed from an antibonding orbital; the equilibrium bond length of the ionic state is therefore expected to be shorter while the vibrational constant ω_e is expected to be larger than that for the IF ($X^1\Sigma^+$) state, as was observed. The actual equilibrium bond length of the ionic state is found by choosing a range of trial values and calculating the quantity $\sum[FCFv'(calcd) - FCFv'(expt)]^2$ for each trial bond length.[27] A curve of this quantity plotted as a function of trial ionic bond length was then obtained. The lowest point of the curve represents the recommended value of the equilibrium bond length for the ionic state. During these FCF calculations, it was assumed that the electronic transition moment is constant over the photoelectron band. This assumption gives an error in the equilibrium bond length of the ionic state of ±0.005Å.[27]

The results obtained for both IF bands are shown in Table 2, where they are compared with the results obtained in the previous HeI PES work[4] in which IF was produced from the F

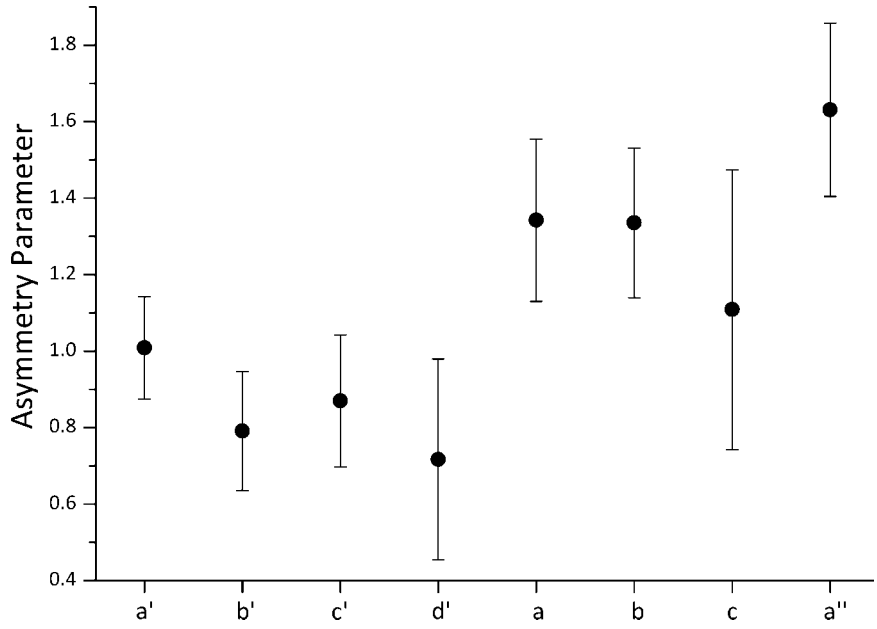

Figure 8. Asymmetry parameter β of the more intense bands shown in Figure 2 at a photon energy of 21.22 eV.

TABLE 2: Ionic Vibrational Constants and Adiabatic and Vertical Ionization Energies for the Two IF Bands Observed in This Work

	IF^+ ($X^2\Pi_{3/2}$)	IF^+ ($^2\Pi_{1/2}$)	IF^+ ($X^2\Pi_{3/2}$)^4	IF^+ ($^2\Pi_{1/2}$)^4
ω_e (cm^{-1})	696 ± 2	687 ± 2	700 ± 30	710 ± 30
$\omega_e x_e$ (cm^{-1})	3.0 ± 0.5	1.2 ± 0.5	10 ± 5	10 ± 5
r_e (Å)	1.836 ± 0.005	1.832 ± 0.005	1.82 ± 0.01	1.82 ± 0.01
AIE (eV)	10.538 ± 0.001	11.244 ± 0.001	10.54 ± 0.01	11.24 ± 0.01
VIE (eV)	10.538 ± 0.001	11.329 ± 0.001	10.62 ± 0.01	11.32 ± 0.01
spin−orbit splitting (cm^{-1})	5690 ± 8		5560 ± 40	

+ ICl reaction. The present results have a much higher precision than the previous ones. This is because the ionization energies of the IF vibrational bands were determined here to within 1 meV. The ionization energy scales for all the PE spectra were calibrated using the known values for the $Ar^+(^2P_{3/2},^2P_{1/2}) \leftarrow Ar(^1S_0)\ (3p)^{-1}$ and $I^+(^1D_2,^3P_2) \leftarrow I(^2P_{3/2})\ (5p)^{-1}$ ionizations. Excellent linearity of the ionization energy scale was ensured by the use of a DAC card with 0.1 mV precision to supply the voltage to the lenses of the spectrometer. Also averaging of the results over many PE spectra allowed determination of the ionization energies of the IF vibrational bands with high precision.

It is notable that the Franck−Condon envelopes for the first two bands of IF are slightly different (Figures 6 and 7) and the derived equilibrium bond lengths for the $X^2\Pi_{3/2}$ and $^2\Pi_{1/2}$ ionic states are also slightly different (Table 2). As these ionic states both arise from the IF $(7\pi)^{-1}$ ionization, their potential curves might be expected to be the same shape and their equilibrium bond lengths and harmonic vibrational constants might be expected to be the same. However, interaction between ionic states (notably spin−orbit interaction between the $^2\Pi_{1/2}$ ionic state and the $^2\Sigma_{1/2}$ ionic state arising from the $(13\sigma)^{-1}$ ionization) would lead to the $X^2\Pi_{3/2}$ and $^2\Pi_{1/2}$ ionic states having slightly different equilibrium constants and potential curves with slightly different shapes. This would explain why slightly different Franck−Condon envelopes are observed for the first two IF bands (Figures 6 and 7).

b. Threshold Photoelectron (TPE) Spectra. To record TPE spectra, the penetrating field analyzer system was tuned to detect near-zero energy (threshold) photoelectrons. The detection of threshold electrons was optimized using the $Ar^+(^2P_{3/2},^2P_{1/2}) \leftarrow Ar(^1S_0)\ (3p)^{-1}$ doublet lines as a guide.[28,29] Figure 9 shows the TPE spectrum of Ar recorded with the optimized values of 100 V for the extractor voltage, $V_1 = 27.7$ V, $V_2 = 13.3$ V, and $V_3 = 3.0$ V. The spectral resolution obtained is about 5 meV as estimated from the full width at half-maximum of the main $Ar^+(^2P_{3/2}) \leftarrow Ar(^1S_0)\ (3p)^{-1}$ band. Argon is a convenient atom to test the performance of the spectrometer since there are high-lying neutral Rydberg states (11s′, 12s′, 13s′, 14s′, etc.) that converge to the $(3p)^{-1}\ ^2P_{1/2}$ ionization limit.[28,29] These excited neutral states can autoionize to the lower-lying $^2P_{3/2}$ ionic state leading to the production of electrons with energies of 3, 38, 62, 81 meV, etc., respectively. At photon energies well away from the threshold, the ratio of the intensities of the argon $Ar^+(^2P_{3/2}) \leftarrow Ar(^1S_0)$ and $Ar^+(^2P_{1/2}) \leftarrow Ar(^1S_0)$ bands is the statistical ratio of 2:1. However, at photon energies slightly above threshold, this ratio increases because of the contribution of the 11s′ autoionizing states which give electrons of 3 meV that enhance the $Ar^+(^2P_{3/2}) \leftarrow Ar(^1S_0)$ channel. The ratio shown in Figure 9 is ~5:1 and indicates that autoionizing states are accessed within about 5 meV above the ionization threshold. Some finite energy electrons will be emitted in the direction of the spectrometer and will also be detected if their energy is within the band-pass of the analyzer. This gives rise to a high-energy tail in the transmission function of the analyzer. As can be seen in Figure 9, there is a small peak at 15.798 eV due to the 12s′ autoionizing state which gives rise to electrons of 38 meV. TPE spectra may therefore contain additional features due to autoionizing states, and this must be taken into account in the interpretation of the spectra. In molecules, this effect may lead to the observation of ionic state vibrational levels outside

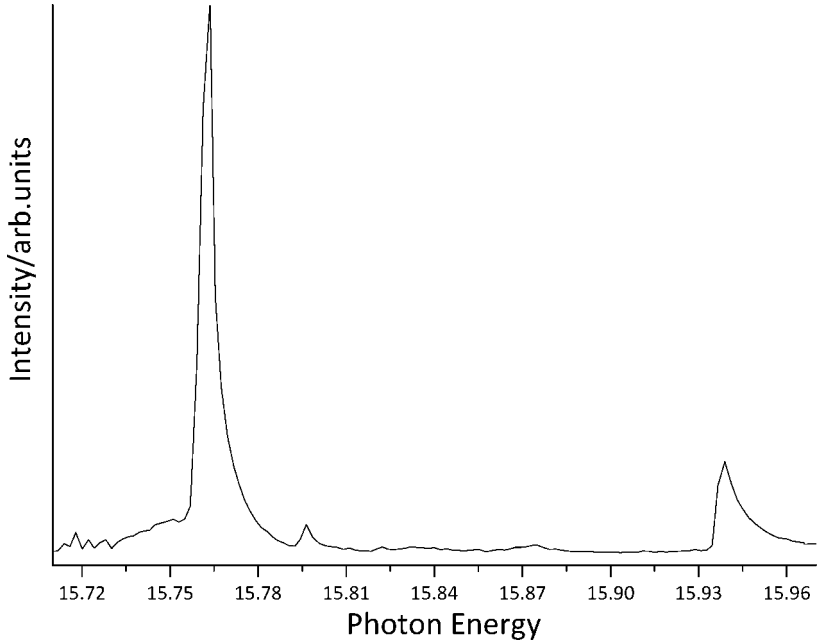

Figure 9. TPE spectrum recorded for argon in the region of the $Ar^+(^2P_{3/2}) \leftarrow Ar(^1S_0)$ and $Ar^+(^2P_{1/2}) \leftarrow Ar(^1S_0)$ $(3p)^{-1}$ ionizations.

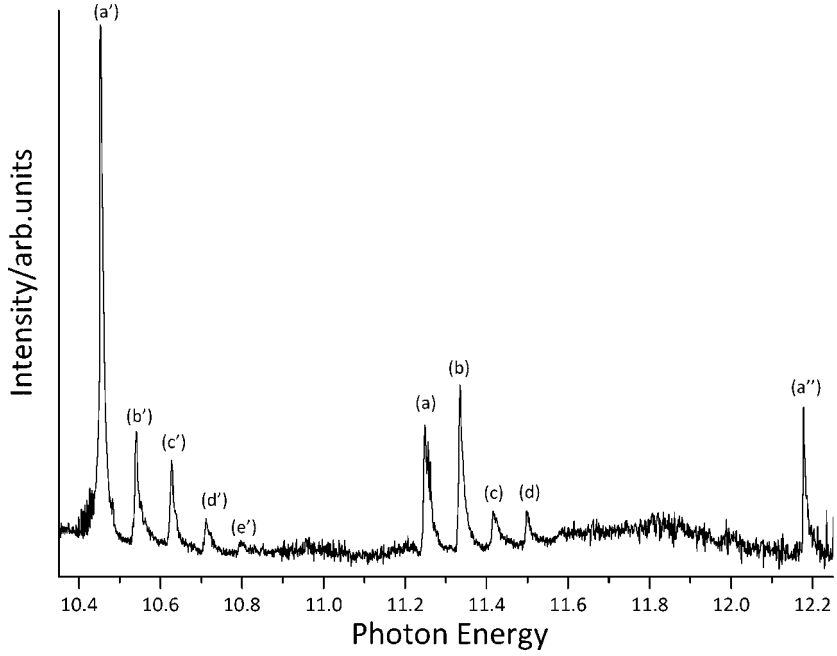

Figure 10. TPE spectrum recorded for the F + CH_2I_2 reaction in the 10.3−12.3 eV photon energy region at a mixing distance of 3 cm.

the normal Franck−Condon region which are enhanced in intensity by autoionization from close-lying Rydberg states.

Figure 10 shows the TPE spectrum recorded for the F + CH_2I_2 reaction in the 10.3−12.3 eV photon energy region at a 3 cm mixing distance. The photon energy scale was calibrated using the known values for $Ar^+(^2P_{3/2},^2P_{1/2}) \leftarrow Ar(^1S_0)$ and $I^+(^1D_2,^3P_2) \leftarrow I(^2P_{3/2})$ ionizations. Comparing Figure 10 with the PE spectrum shown in Figure 3, it can be seen that better resolution is obtained for the TPE spectra, and as expected, different relative intensities of the bands are observed. All the atomic I features have increased in intensity with respect to the IF bands compared to that of the PE spectra. This is particularly the case for band (a′), corresponding to the first iodine atom ionization, $I^+(^3P_2) \leftarrow I(^2P_{3/2})$. This is probably due to an autoionization resonance as for the case of the $Ar^+(^2P_{3/2}) \leftarrow Ar(^1S_0)$ ionization. In the photoionization work of Berkowitz et al.,[30] the *ns* Rydberg series converging to the $I^+(^3P_0)$ limit of atomic I has an $n = 8$ component at an excitation energy equal to 10.4535 eV. This Rydberg level is only 2.5 meV above the $I^+(^3P_2) \leftarrow I(^2P_{3/2})$ limit, and therefore it can autoionize, giving electrons of 2.5 meV that enhance the $I^+(^3P_2) \leftarrow I(^2P_{3/2})$ channel. In a photoabsorption study, Sarma and Joshi[31] observed a different *ns* series converging to the $^3P_1$ limit assigned as $(^3P_1)ns[1]_{3/2}$ in the J$_c$l coupling scheme. The $n = 8$ state of this series has an excitation energy of 10.4596 eV, 8.6 meV above the $I^+(^3P_2) \leftarrow I(^2P_{3/2})$ ionization energy at 10.451 eV. It can also autoionize to the $I^+(^3P_2)$ state enhancing the $I^+(^3P_2) \leftarrow I(^2P_{3/2})$ TPE intensity.

Comparison of Figures 3 and 10 also shows that the relative intensities of the $IF^+ \leftarrow IF$ bands are similar in both the TPE and PE spectra. In particular, higher vibrational members of the first IF photoelectron band are not observed in the TPE

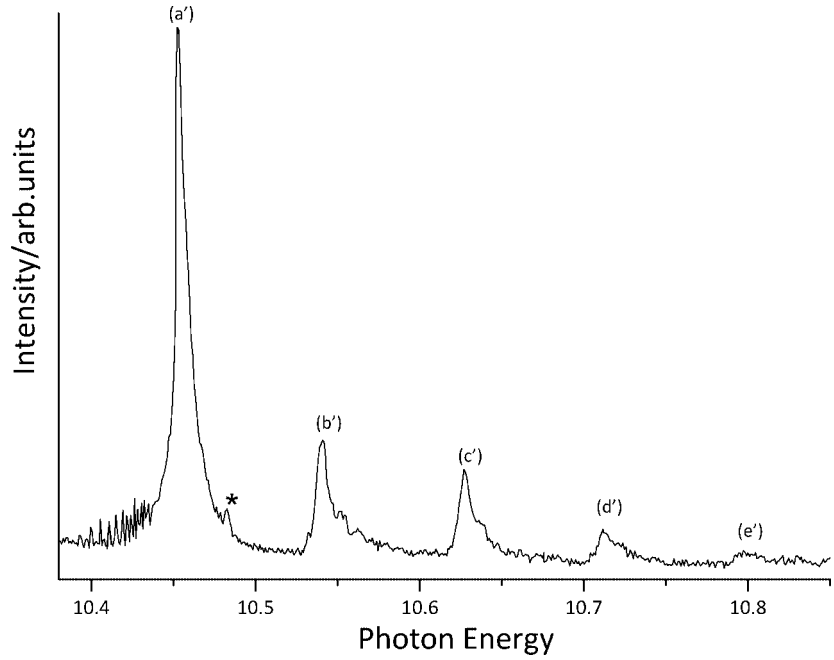

Figure 11. TPE spectrum showing the $I^+(^3P_2) \leftarrow I(^2P_{3/2})$ and the IF $(X^2\Pi_{3/2}) \leftarrow IF(X\ ^1\Sigma)$ bands.

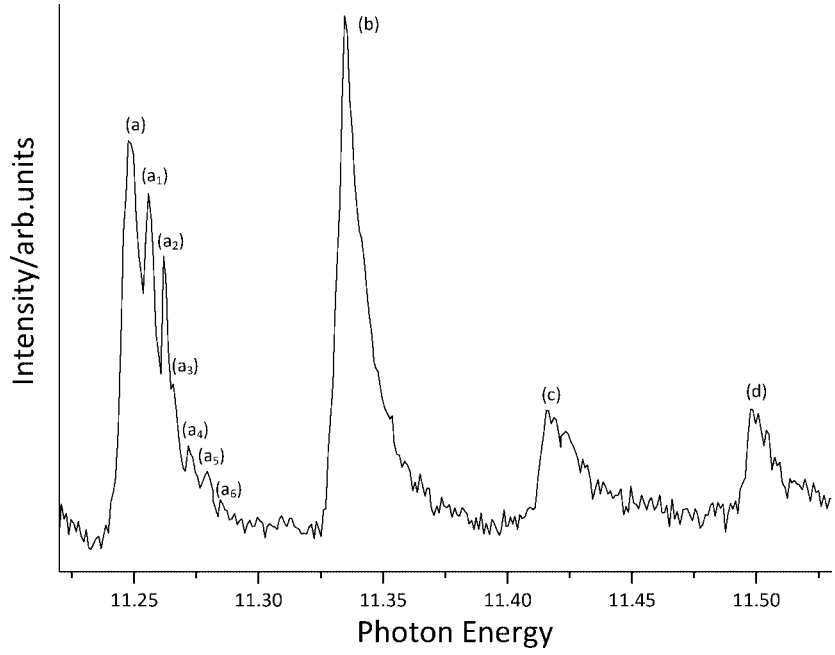

Figure 12. TPE spectrum showing the $I^+(^3P_{0,1}) \leftarrow I(^2P_{3/2})$ and $IF^+(^2\Pi_{1/2}) \leftarrow IF(X\ ^1\Sigma)$ bands. Bands (a) and (b) are overlapped I and IF features, whereas bands (c) and (d) are IF vibrational components (see text).

spectrum in the "non-Franck−Condon region" between the $IF^+(X^2\Pi_{3/2}) \leftarrow IF(X^1\Sigma)$ and $IF^+(^2\Pi_{1/2}) \leftarrow IF(X^1\Sigma)$ bands, indicating an absence of significant autoionization to these vibrational states.

An expanded scan in the energy region of the $I^+(^3P_2) \leftarrow I(^2P_{3/2})$ and the $IF^+(X^2\Pi_{3/2}) \leftarrow IF(X^1\Sigma)$ bands, 10.40−10.85 eV, is shown in Figure 11. A small band can be observed of about 5% the intensity of the $I^+(^3P_2) \leftarrow I(^2P_{3/2})$ band and 31 meV higher in photon energy (it is denoted by an "*" in Figure 11). This could be associated with a high-lying neutral Rydberg state that autoionizes to the lower-lying $I^+(^3P_2)$ state. Berkowitz et al.[30] assigned the $n = 8$ state of an *ns* series converging to the $^3P_1$ limit at a photon energy of 10.4827 eV. Sarma and Joshi[31] reported two *ns* series converging to the $^3P_1$ limit assigned as $(^3P_1)ns[1]_{1/2}$ and $(^3P_1)ns[1]_{3/2}$. The $(^3P_1)8s[1]_{1/2}$ Rydberg state has an excitation energy of 10.4830 meV, which is comparable with the result obtained by Berkowitz et al.[30] Autoionization of this state to the lower-lying $I^+(^3P_2)$ ionic state would give photoelectrons of 31 meV.

Figure 12 shows an expanded scan of the energy region 11.22−11.52 eV containing the $I^+(^3P_{1,0}) \leftarrow I(^2P_{3/2})$ and the $IF^+(X^2\Pi_{1/2}) \leftarrow IF(X\ ^1\Sigma)$ bands. Associated with band (a), two intense sharp peaks (a_1 and a_2) and four smaller peaks (a_3, a_4, a_5, and a_6) can be seen. As noted above, band (a) has contributions from both I and IF. It is possible that the two contributions are resolved, but the fact that band (a_1) is sharp (2−3 meV) may indicate that it is associated with an autoionizing I atom Rydberg state. Moreover, its photon energy (∼11.255 eV) is too high to be assigned as the $I^+(^3P_0) \leftarrow I(^2P_{3/2})$ band at 11.251 eV. This may suggest that the wide band

TABLE 3: Comparison between the Measured Positions of the Vibrational Components of the Two IF PE Bands As Obtained in PE and TPE Spectra

v^+	IF^+ ($X^2\Pi_{3/2}$) PES	IF^+ ($X^2\Pi_{3/2}$) TPES	IF^+ ($^2\Pi_{1/2}$) PES	IF^+ ($^2\Pi_{1/2}$) TPES
0	10.539 ± 0.001	10.539 ± 0.001	11.244 ± 0.001	11.245 ± 0.001
1	10.625 ± 0.001	10.625 ± 0.002	11.329 ± 0.001	11.333 ± 0.001
2	10.709 ± 0.001	10.709 ± 0.002	11.413 ± 0.001	11.413 ± 0.001
3	10.792 ± 0.003	10.793 ± 0.002	11.497 ± 0.002	11.496 ± 0.002

(a) (5−6 meV) has contributions from overlapping I and IF bands, while the first sharp peak (a_1) could be associated with 4 meV electrons arising from autoionization of an I atom Rydberg state. CIS spectra on the $I^+(^3P_2) \leftarrow I(^2P_{3/2})$ ionization band have been recorded, and they will be reported in a future article. A first analysis of these spectra shows several Rydberg states converging to the $I^+(^3P_1) \leftarrow I(^2P_{3/2})$ limit at 11.330 eV[32,33] in the 11.0−11.3 eV photon energy region. This again suggests that the band (a) is an overlap of I and IF bands, while the other sharp features, (a_1) to (a_6), are associated with I atom Rydberg autoionizing resonances. Berkowitz et al.[30] found one *ns* and one *nd* series converging to the ($^3P_1$) limit with several resonances in the 11.255−11.285 eV photon energy region. The same Rydberg series but with slightly different photon energies were reported by Gu et al.[34] and assigned as $(^3P_1)ns[1]_{3/2}$ and $(^3P_1)nd[2]_{5/2}$ resonances from the $I(^2P_{3/2})$ ground state. Autoionization of $(^3P_1)16d[2]_{5/2}$ and $(^3P_1)18s[1]_{3/2}$ I atom Rydberg states to the $I^+(^3P_0)$ ionic state can be associated with bands (a_1) and (a_2) at 11.2565 and 11.2606 eV,[34] respectively. Features (a_3, a_4, a_5 and a_6) may also be assigned as overlapping autoionization features from higher *n* Rydberg states of both *ns* and *nd* series.[30,34]

Table 3 compares the ionization energies obtained from PE and TPE spectra for the $IF^+(X^2\Pi_{3/2}) \leftarrow IF(X^1\Sigma)$ and $IF^+(X^2\Pi_{1/2}) \leftarrow IF(X^1\Sigma)$ bands. The agreement between the two sets of measurements is in general excellent. This is significant since their respective uncertainties arise from different sources. In the case of the PE spectra, the linearity and precision of the energy calibration depends upon the voltages applied to the spectrometer, notably the voltage applied to the third lens element. This voltage has a precision of about 0.2 mV. The peak position of each photoelectron band is determined from a Gaussian fit with a precision of about 0.5−1.0 meV for an intense band. Furthermore, in this work the ionization energy position for each band was averaged over the results obtained from many PE spectra. Therefore, the error associated with the ionization energy of any of the intense bands is estimated to be 1 meV. On the other hand, for the case of the TPE spectra the voltages applied to the spectrometer are held constant and the photon energy is swept linearly. The photon energy calibration of the monochromator is obtained with a precision of about 1 meV, while the TPE peak position is obtained with a precision of about 0.5 meV. The error associated with the photon energy position of a TPE band is thus estimated to be between 1 and 2 meV.

The same ionization energy values are obtained for three of the four $IF^+(X^2\Pi_{3/2},v^+) \leftarrow IF(X^1\Sigma,v'' = 0)$ vibrational components ($v^+ = 0, 1, 2$). For the fourth ($v^+ = 3$), there is a difference of 1 meV, which is within experimental error (Table 3). Also, for three of the four $IF^+(X^2\Pi_{1/2},v^+) \leftarrow IF(X^1\Sigma,v'' = 0)$ vibrational components the same ionization energy values are obtained with a difference of 4 meV for $v^+ = 1$ (this contributes to band (b) in Figure 12). The value of 11.333 eV obtained in the TPE measurement is too high to be associated with either IF or I. A possible explanation is a contribution from autoionizing I atom Rydberg states. Berkowitz et al.[30] reported two *ns* series converging to the $^1D_2$ limit with excitation energies to the $n = 8$ Rydberg states close to 11.333 meV. The lower photon energy side of a TPE band has normally a sharp increase corresponding to the energy width of the incident photon beam, in this work about 3−4 meV from the bottom to the top of the peak. This value is 10 meV for band (b). This can be explained if band (b) in the TPE spectrum arises from the overlap of IF and I contributions at lower photon energy and contributions from one or two autoionizing I atom Rydberg states at higher photon energy.

In summary, this work investigated IF and I bands in the ionization energy region 10.0−15.0 eV by PES. Their relative intensities were measured and, where IF and I bands overlapped, their relative contributions were established. This was not done in the initial study.[4] This work has led to improved adiabatic ionization energies (AIEs) and VIEs of the $IF^+(X^2\Pi_{3/2}) \leftarrow IF(X^1\Sigma^+)$ and $IF^+(^2\Pi_{1/2}) \leftarrow IF(X^1\Sigma^+)$ ionizations and improved spectroscopic constants ω_e, $\omega_e x_e$, and r_e for the two IF ionic states $X^2\Pi_{3/2}$ and $^2\Pi_{1/2}$.

Comparison of the TPE and PE spectra for IF and I shows that no difference can be seen between the vibrational envelopes of the two observed IF bands. Unlike TPE spectra recorded for other diatomic halogens,[5–8] no extra vibrational structure is observed in the TPE spectrum of IF, particularly in the "Franck−Condon gap" between the two observed bands. The extra structure seen in the TPE spectra, notably associated with bands (a) and (a′), and the position of band (b), which is higher in the TPE spectrum compared to its position in the PE spectrum by 4 meV, can be attributed to autoionization contributions from know I atom Rydberg states.

Acknowledgment. We are grateful to EPSRC for supporting this work. We also thank Dr. N. Zema and the technical staff of the Polar beamline (4.2R) at Elettra, Trieste, for help and advice. M.E. and S.B. thank the EU Early Stage Research Training Network (SEARCHERS) for financial support.

References and Notes

(1) (a) Davis, S. J.; Hanko, L.; Wolf, P. L. *J. Chem. Phys.* **1985**, *82*, 4831. (b) Davis, S. J.; Woodward, A. M. *J. Phys. Chem.* **1991**, *95*, 4610.

(2) (a) Helms, C. A.; Hanko, L.; Healey, K.; Hager, G.; Perram, G. P. *J. Appl. Phys.* **1989**, *66*, 6093. (b) Kane, K. Y.; Eden, J. G. *IEEE J. Quantum Electron.* **1990**, *26*, 1620.

(3) (a) Gavrikov, V. F.; Dvoryankin, A. N.; Stepanov, A. A.; Shmelev, A. K.; Shcheglov, V. A. *J. Russ. Laser Res.* **1994**, *15*, 177. (b) Trautmann, M.; Trickl, T. R.; Wanner, J. *Ber. Bunsen-Ges Phys. Chem.* **1982**, *86*, 841.

(4) Colbourn, E. A.; Dyke, J. M.; Fayad, N. K.; Morris, A. *J. Electron Spectrosc. Relat. Phenom.* **1978**, *14*, 443.

(5) Cormack, A. J.; Yencha, A. J.; Donovan, R. J.; Lawley, K. P.; Hopkirk, A.; King, G. C. *Chem. Phys.* **1996**, *213*, 439.

(6) Yencha, A. J.; Hopkirk, A.; Hiraya, A.; Donovan, R. J.; Goode, J. G.; Maier, R. R. J.; King, G. C.; Kvaran, A. *J. Phys. Chem.* **1995**, *99*, 7231.

(7) Yencha, A. J.; Lopes, M. C. A.; King, G. C. *Chem. Phys. Lett.* **2000**, *325*, 559.

(8) Yencha, A. J.; Malins, A. E. R.; King, G. C. *Chem. Phys. Lett.* **2003**, *370*, 756.

(9) Innocenti, F.; Zuin, L.; Costa, M. L.; Dias, A. A.; Morris, A.; Stranges, S.; Dyke, J. M. *J. Chem. Phys.* **2007**, *126*, 154310.

(10) Dyke, J. M.; Gamblin, S. D.; Morris, A.; Wright, T. G.; Wright, A. E.; West, J. B. *J. Electron Spectrosc. Relat. Phenom.* **1998**, *97*, 5.

(11) Dyke, J. M.; Gamblin, S. D.; Morris, A.; Wright, T. G.; Wright, A. E.; West, J. B. *J. Phys. B: At. Mol. Opt. Phys.* **1999**, *32*, 2763.

(12) Innocenti, F.; Zuin, L.; Costa, M. L.; Dias, A. A.; Goubet, M.; Morris, A.; Oleriu, R. I.; Stranges, S.; Dyke, J. M. *Mol. Phys.* **2007**, *105*, 755.

(13) Cvejanovic, S.; Read, F. H. *J. Phys. B: At. Mol. Opt. Phys.* **1974**, *7*, 1180.

(14) Guyon, P. M.; Spohr, R.; Chupka, W. A.; Berkowitz, J. *J. Chem. Phys.* **1976**, *65*, 1650.
(15) Baer, T.; Guyon, P. M. *J. Chem. Phys.* **1986**, *85*, 4368.
(16) Worsdorfer, U.; Heydtmann, H. *Ber. Bunsen-Ges. Phys. Chem.* **1989**, *93*, 1132.
(17) Andrews, L.; Dyke, J. M.; Jonathan, N.; Keddar, N.; Morris, A. *J. Phys. Chem.* **1984**, *88*, 1950.
(18) de Leeuw, D. M.; Mooyman, R.; de Lange, C. A. *Chem. Phys. Lett.* **1978**, *54*, 26.
(19) National Institute of Standards and Technology. Physics Laboratory Physical Reference Data. http://physics.nist.gov/PhysRefData.
(20) (a) Huffman, R. E.; Larrabee, J. C.; Tanaka, Y. *J. Chem. Phys.* **1967**, *47*, 856. (b) Huffman, R. E.; Larrabee, J. C.; Tanaka, Y. *J. Chem. Phys.* **1968**, *48*, 3835.
(21) Dyke, J. M.; Jonathan, N.; Morris, A. *Int. Rev. Phys. Chem.* **1982**, *2*, 3.
(22) Berkowitz, J.; Goodman, G. L. *J. Chem. Phys.* **1979**, *71*, 1754.
(23) Eland, J. H. D. *Photoelectron Spectroscopy*; Butterworths: Oxford, 1984.
(24) Huber, K. P.; Herzberg, G. *Constants of Diatomic Molecules*; van Nostrand Reinhold: New York, 1979.
(25) Durie, R. A. *Can. J. Phys.* **1966**, *44*, 337.
(26) McGurk, J. C.; Flygare, W. H. *J. Chem. Phys.* **1973**, *59*, 5742.
(27) Dyke, J. M. *J. Chem. Soc., Faraday Trans. 2* **1987**, *83*, 67.
(28) King, G. C.; Zubek, M.; Rutter, P. M.; Read, F. H. *J. Phys. E* **1987**, *20*, 440.
(29) Hall, R. I.; McConkey, A.; Ellis, K.; Dawber, G.; Avaldi, L.; MacDonald, M. A.; King, G. C. *Meas. Sci. Technol.* **1992**, *3*, 316.
(30) Berkowitz, J.; Batson, C. H.; Goodman, G. L. *Phys. Rev. A: At., Mol., Opt. Phys.* **1981**, *24*, 149.
(31) Sarma, V. N.; Joshi, Y. N. *Can. J. Phys.* **1983**, *61*, 1434.
(32) Minnhagen, L. *Ark. Fys.* **1961**, *21*, 415.
(33) Martin, W. C.; Corliss, C. H. *J. Res. Natl. Bur. Stand. (U.S.)* **1960**, *64A*, 443.
(34) Gu, Y. Y.; Chojacki, A. M.; Zietkiewicz, C. J.; Senin, A. A.; Eden, J. G. *J. Chem. Phys.* **2003**, *119*, 12342.

JP803141C